Available online at www.sciencedirect.com
ScienceDirect
Global and Planetary Change 59 (2007) 110–125
GLOBAL AND PLANETARY CHANGE
www.elsevier.com/locate/gloplacha

Evaluating digital elevation models for glaciologic applications: An example from Nevado Coropuna, Peruvian Andes

Adina E. Racoviteanu [a,b,*], William F. Manley [b], Yves Arnaud [c], Mark W. Williams [a,b]

[a] Department of Geography, University of Colorado, CB 260, Boulder CO 80309, USA
[b] Institute of Arctic and Alpine Research, University of Colorado, CB 450, Boulder CO 80309, USA
[c] Institut de Recherche pour le Développement, UR GREAT ICE, Laboratoire de Glaciologie et Géophysique de l'Environnement, 38402 Saint Martin d'Hères Cedex, France

Available online 10 January 2007

Abstract

This paper evaluates the suitability of readily available elevation data derived from recent sensors – the Advanced Spaceborne Thermal Emission and Reflection Radiometer (ASTER) and the Shuttle Radar Topography Mission (SRTM) – for glaciological applications. The study area is Nevado Coropuna (6426 m), situated in Cordillera Ampato of Southern Peru. The glaciated area was 82.6 km^2 in 1962, based on aerial photography. We estimate the glacier area to be ca. 60.8 km^2 in 2000, based on analysis of the ASTER L1B scene.

We used two 1:50,000 topographic maps constructed from 1955 aerial photography to create a digital elevation model with 30 m resolution, which we used as a reference dataset. Of the various interpolation techniques examined, the TOPOGRID algorithm was found to be superior to other techniques, and yielded a DEM with a vertical accuracy of ±14.7 m. The 1955 DEM was compared to the SRTM DEM (2000) and ASTER DEM (2001) on a cell-by-cell basis. Steps included: validating the DEM's against field GPS survey points on rock areas; visualization techniques such as shaded relief and contour maps; quantifying errors (bias) in each DEM; correlating vertical differences between various DEM's with topographic characteristics (elevation, slope and aspect) and subtracting DEM elevations on a cell-by-cell basis.

The RMS error of the SRTM DEM with respect to GPS points on non-glaciated areas was 23 m. The ASTER DEM had a RMS error of 61 m with respect to GPS points and displayed 200–300 m horizontal offsets and elevation 'spikes' on the glaciated area when compared to the DEM from topographic data.

Cell-by-cell comparison of SRTM and ASTER-derived elevations with topographic data showed ablation at the toes of the glaciers (−25 m to −75 m surface lowering) and an apparent thickening at the summits. The mean altitude difference on glaciated area (SRTM minus topographic DEM) was −5 m, pointing towards a lowering of the glacier surface during the period 1955–2000. Spurious values on the glacier surface in the ASTER DEM affected the analysis and thus prevented us from quantifying the glacier changes based on the ASTER data.

Keywords: Digital Elevation Model (DEM); Geographic Information Systems (GIS); Andes; Glaciology; DEM generation; ASTER; SRTM

1. Introduction

Digital elevation models (DEM's) are beginning to see wide use in glaciological applications. Some studies have used DEM's to extract components of glacier

* Corresponding author. Department of Geography, University of Colorado, CB 260, Boulder CO 80309, USA. Tel.: +1 303 492 5546; fax: +1 303 492 6388.
E-mail address: racovite@colorado.edu (A.E. Racoviteanu).

0921-8181/$ - see front matter © 2006 Elsevier B.V. All rights reserved.
doi:10.1016/j.gloplacha.2006.11.036

topography (slope and aspect), which were then combined with satellite images to map glacier areas (Klein and Isacks, 1996; Duncan et al., 1998; Sidjak, 1999; Kääb et al., 2002a; Paul et al., 2002). In addition, DEM's have been used as tools to derive hypsometry maps at different time steps and to quantify vertical surface changes on glaciers in remote areas, as indirect measurements of mass balance (Khalsa et al., 2004; Berthier et al., 2004).

Several studies have explored ways to assess glacier mass balance and volumetric change by using time series of digital elevation data. For example, Etzelmüller (2000), Etzelmüller and Björnsson (2000) and Etzelmüller et al. (1993) discussed GIS techniques to quantify changes in elevation, terrain roughness, glacier hypsometry and flow patterns using grid-based DEM's. Rentsch et al. (1990), Vignon et al. (2003) and Rivera and Casassa (1999) estimated changes in glacier volume and mass balance based on reference elevations from topographic data.

The availability of new remote sensing platforms with high resolution, global coverage and low costs provide the potential to calculate glacier mass balances in remote areas with little existing glacial information, such as the Andes of South America. Two of the new sensors are the Advanced Spaceborne Thermal Emission and Reflection Radiometer (ASTER) sensor and the Shuttle Radar Topography Mission (SRTM). The ASTER sensor acquires simultaneous stereo images from different directions, suitable for generation of DEM's. Glaciologists would like to evaluate changes in glacial mass balance over time by comparing changes in DEM properties acquired at different times (Etzelmüller, 2000). Efforts are being undertaken to provide accuracy assessments of the new DEM's from SRTM and ASTER imagery. For instance, ASTER-derived DEM's (30 m resolution) have been validated at several sites (e.g. Welch et al., 1998; Lang and Welch, 1999; Kääb, 2002; Hirano et al., 2003). The recently released SRTM-3 (90 m resolution) datasets have been evaluated only at a few study sites, on non-glaciated terrain (e.g. Falorni et al., 2003; Rabus et al., 2003). Therefore, it is unclear if the data available to glaciologists from these new remote sensing instruments provide sufficient spatial and temporal resolution to detect a glacial signal without extensive calibration.

Combining these new satellite-derived DEM's with DEM's constructed from topographic maps has the potential to extend the time series of glacial change over many decades. This ability to construct glacial mass balances over many decades is particularly well-suited to remote areas such as the Andes where there is little historical research in glaciology. In such areas, digitized elevation contours from old topographic maps still constitute a ready source of historical data on glacier elevation and area. However, there is no established interpolation method especially suitable for creating continuous elevation data from these topographic maps for accurate representation of glacier terrain. The accuracy of various techniques to construct DEM's from digitized contour data has been addressed in GIS literature, such as Burrough and McDonnell (1998) and Wood and Fisher (1993), but the glaciological community has yet to agree on a suitable interpolation method. For instance, Etzelmüller and Björnsson (2000) used an Inverse Distance Weighted (IDW) interpolator to create a continuous surface from radar profile lines on a glacier. Other authors (e.g. Mennis and Fountain, 2001) chose a spline interpolation for representation of glacier and sub-glacier topography. Alternatively, Gratton et al. (1990) chose a Triangular Irregular Network (TIN) derived from digitized contours to represent rugged glacier topography at the Columbia Icefield. The choice of interpolation method depends on terrain topography and the type of data analysis needed. So far, only a few glaciological studies (e.g. Cogley and Jung-Rothenhausler, 2004) provided a careful quantitative evaluation of interpolation accuracy over glaciated area using ground data. At present we do not know how sensitive glacial mass balance calculations are to the type of interpolation method used to create glacier elevation surfaces.

Here we assess the suitability of readily available SRTM and ASTER datasets for mass balance studies at a remote mountain area in the Peruvian Andes. The SRTM DEM's released by USGS and the ASTER DEM's generated at the EROS Data Center constitute information in the public domain available to all glaciologists. Our objectives are: 1) to evaluate the suitability of various interpolation techniques to construct DEM's for glaciological studies; 2) to assess elevation differences between DEM's from satellite data and the DEM from topographic data, 3) to identify the spatial distribution of these errors with respect to topographic characteristics (elevation, slope and aspect) and 4) to ultimately distinguish a glacier signal from multi-temporal DEM's.

2. Study area

Our study area is Nevado Coropuna (Fig. 1), situated in the volcanic Cordillera Ampato in Southern Peru (15°24′–15°51′S latitude and 71°51′–73°00′W longitude) (Fig. 2). The Ampato range consists of 93 glaciers,

Fig. 1. Nevado Coropuna (6426 msl), Peruvian Andes.

with an estimated average glacier thickness of ~35 m and a total glaciated area of 146.73 km^2 based on 1962 aerial photography (Ames et al., 1989). Nevado Coropuna is the highest peak in Cordillera Ampato, ranging from ~4600 m at the base (Lake Pallacocha) to over 6400 m at the main summit, with gentle sloping lava flows and glaciated terrain. There have been no comprehensive field measurements of glacial properties on Nevado Coropuna until recently. The only glacier mapping was carried out by Ames et al. (1989) who reported a glaciated area of 82.6 km^2 for Nevado Coropuna based on planimetric analysis of 1962 aerial photography. This manuscript fills this gap and complements two ice-core-drilling expeditions conducted on Coropuna in 2003 by l'Institut de Recherche pour le Développement, France (GREAT ICE project) and the Ice Core Paleoclimatology Research Group at the Byrd Polar Research Center, Ohio State University. Results from these paleoclimatic studies will provide an isotopic record for the region, which can help understand the climatic variability in the region and assess present-day glacier fluctuations in the area.

3. Methods

3.1. Field data collection

In June and August 2003, GPS points were obtained using a handheld Garmin Etrex GPS unit in navigation mode on both rock and glaciated areas (Fig. 2). The light and portable Garmin was preferred over the bigger Trimble Pathfinder unit. However, a disadvantage of the navigation-mode GPS is that it cannot be differentially corrected. The accuracy of the Garmin unit was tested at Green Lakes Valley Long-Term Ecological Research (LTER) study site in Colorado (Ackerman et al., 2001). Horizontal errors of measurements taken with the Garmin unit were within 3.9 m of the differentially corrected data obtained with the Trimble Pathfinder (Ackerman et al., 2001). As a rule of thumb, we consider the vertical accuracy of the Garmin unit to be about 1.5 times bigger than horizontal errors (~10 m). The GPS elevations referenced to the WGS84 ellipsoid were converted to orthometric heights (heights above the EGM96 geoid) by subtracting geoid heights calculated for each point based on latitude and longitude (Rapp, 1996).

3.2. Construction of the DEM from topographic data

Two 1:50,000 topographic maps, constructed from 1955 aerial photography by Instituto Geográfico Nacional (IGN) of Peru were needed to cover the study site. The maps used Provisional South American Datum of 1956 for Peru, and elevations were referenced to mean sea level. The maps were scanned and georeferenced based on UTM grids with a positional accuracy (calculated as root mean square error in the X and Y

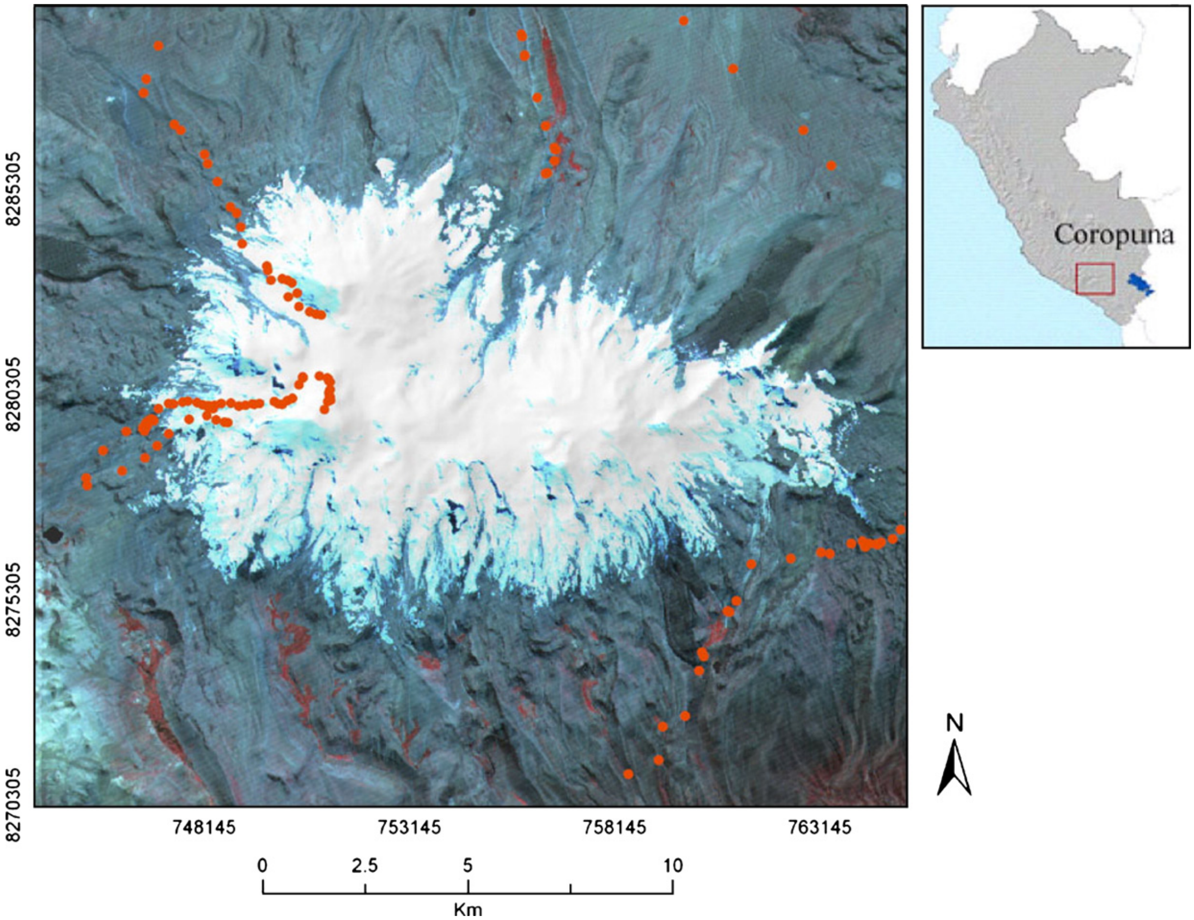

Fig. 2. Location map of the study area. The ASTER Level 1A image from July 2001 is draped over a shaded relief map of the topographic DEM. Also shown are GPS transects surveyed in the field (red dots).

coordinates) of 4 m. Contour lines with 25 m spacing were digitized on screen, and attributed the corresponding elevation values read from the topographic map. Additional GIS layers digitized from the topographic maps included lakes, streams, spot heights and the 1955 snowline.

We examined common interpolation routines to create continuous data from the digitized contours. These included: Inverse Distance Weighted (IDW), Splines (TOPOGRID) and Triangulated Irregular Network (TINs). The IDW method estimates the Z value of an unknown point based on a distance-weighted average of elevation points within a neighborhood (Burrough and McDonnell, 1998). Spline techniques use a piecewise function to fit a curve through all the data points. The TOPOGRID algorithm is a more sophisticated spline technique (thin plate spline) that fits a smoothing surface through the data points to minimize artifacts (excessively high or low spurious values) (Burrough and McDonnell, 1998). TOPOGRID interpolates directly from the contour lines by determining areas of steepest slope and generating terrain morphology. Ancillary hydrologic data (streams and lakes) are used to define drainage based on the ANUDEM algorithm for hydrologic modeling described by Hutchinson (1988). Triangulated Irregular Network (TIN) data structures are terrain models represented by continuous triangular facets that store elevation at irregularly spaced nodes (Burrough and McDonnell, 1998).

3.3. SRTM and ASTER datasets

The Shuttle Radar Topography Mission (SRTM) acquired data in February 2000, from which digital elevation models are created (Rabus et al., 2003). Preliminary elevation datasets with 90 m resolution ('SRTM-3') were recently released for South America. An elevation dataset (1-degree latitude by 1-degree longitude) was obtained for the study area, referenced to UTM projection and resampled to 30 m resolution. Elevations are in meters, referenced to the EGS84 EGM96 geoid (USGS, 2003).

Two ASTER scenes acquired by along-track stereo channel (3), with nadir (3n) and aft-viewing (3b) orientations (Kääb, 2002) were obtained from the Land Processes DAAC at EROS Data Center: one Level 1 B scene from October 2000 and one Level 1A scene from July 2001. The cloud-free 2001 ASTER scene, shown in Fig. 2, was used to extract a DEM using automated stereo auto-correlation procedures at the USGS EROS Data Center. Ground control points (GCP's) were required to obtain an "absolute" ASTER DEM (where locations are fitted to UTM coordinate system and elevations referenced to mean sea level) (Hirano et al., 2003). Eight GCP's were digitized from the topographic maps at river crossings, spot elevations and road intersections and identified on the 3n and 3b bands of the Aster image, following the protocol of Hirano et al. (2003) and Khalsa et al. (2004). The resulting ASTER-derived DEM had 30 m post spacing.

Various ASTER scenes were evaluated to find the one that provided the best glacial extent, based on image contrast and minimal snow coverage. We used the ASTER L1B scene obtained in October 2000 (end of the dry season in the Andes) to delimitate the glacier outline. An unsupervised ISODATA clustering classification (Aniya et al., 1996; Paul, 2001) was performed using ASTER VNIR channels (1, 2 and 3) to delimitate the ice extent. The resulting raster image was converted to polygon coverage and was visually checked to ensure correspondence with glaciated areas on the color composite image.

3.4. DEM validation and comparison

We focused on evaluating errors in the vertical coordinate (Z), estimated as root mean square errors (RMSEz). The Z coordinate is the only unconstrained value, since X and Y coordinates were used to locate corresponding grid cells in all DEM's. Moreover, elevation is the coordinate of interest in glaciological applications because changes in surface elevation over time can be an indicator of mass balance changes (Etzelmüller, 2000). The RMSEz of the various interpolated methods was calculated with respect to evenly distributed spot elevations digitized from topographic maps. The RMSEz of the SRTM and ASTER DEM's was calculated with respect to GPS points from non-glaciated areas. Visualization techniques (shaded relief maps, elevation contours and slope maps) were used to examine the representation of topography in each DEM.

Difference maps were constructed by subtracting the DEM from topographic data from both the ASTER and SRTM-derived DEM's on a cell-by-cell basis. We examined correlations between vertical differences and topographic characteristics (elevation, slope and aspect). Errors on the non-glaciated areas ('bias') were quantified by performing trend surface analyses on the difference maps. After removing the bias, we examined the remaining elevation differences on glaciated areas to distinguish a glacier signal using histograms, summary statistics and color maps of the height differences.

4. Results and discussion

4.1. Topographic interpolation results

An examination of the RMSEz values for DEM's derived from topographic data (Table 1) shows that no interpolation method performed perfectly. The vertical accuracy of the DEM created with the TOPOGRID algorithm was 14.7 m based on 61 spot elevations. The other interpolation methods yielded RMSEz values that ranged from ~21 to 24 m, which is 30–40% greater than the TOPOGRID algorithm (Table 1). A one-way analysis of variance (ANOVA) test showed that there was a significant difference in the DEM's created with various interpolation methods at the 0.1 significance level (p-value = 0.07). The RMSEz of 14.7 m using the TOPOGRID algorithm is only slightly bigger than half of the contour interval (25 m), which is considered an acceptable vertical accuracy for DEM's derived from topographic maps (Cogley and Jung-Rothenhausler, 2004).

All DEM's constructed from contours lines display 'terracing' effects due to denser sampling along the contour lines, because points closer to the contour lines are interpolated using the same elevation values (Burrough and McDonnell, 1998). The terracing effect is most visible on flat surfaces where contours are spread apart, and is most severe when using local interpolator

Table 1
Evaluation of different interpolation methods used to construct DEM's from the topographic maps

Interpolation method	RMSEz spot elevations (m)	Terracing	Other artifacts
TOPOGRID	14.7	Light	Cones
IDW	24.2	Severe	No
TIN	22.0	No	Triangulation
SPLINE	21.1	Moderate	No

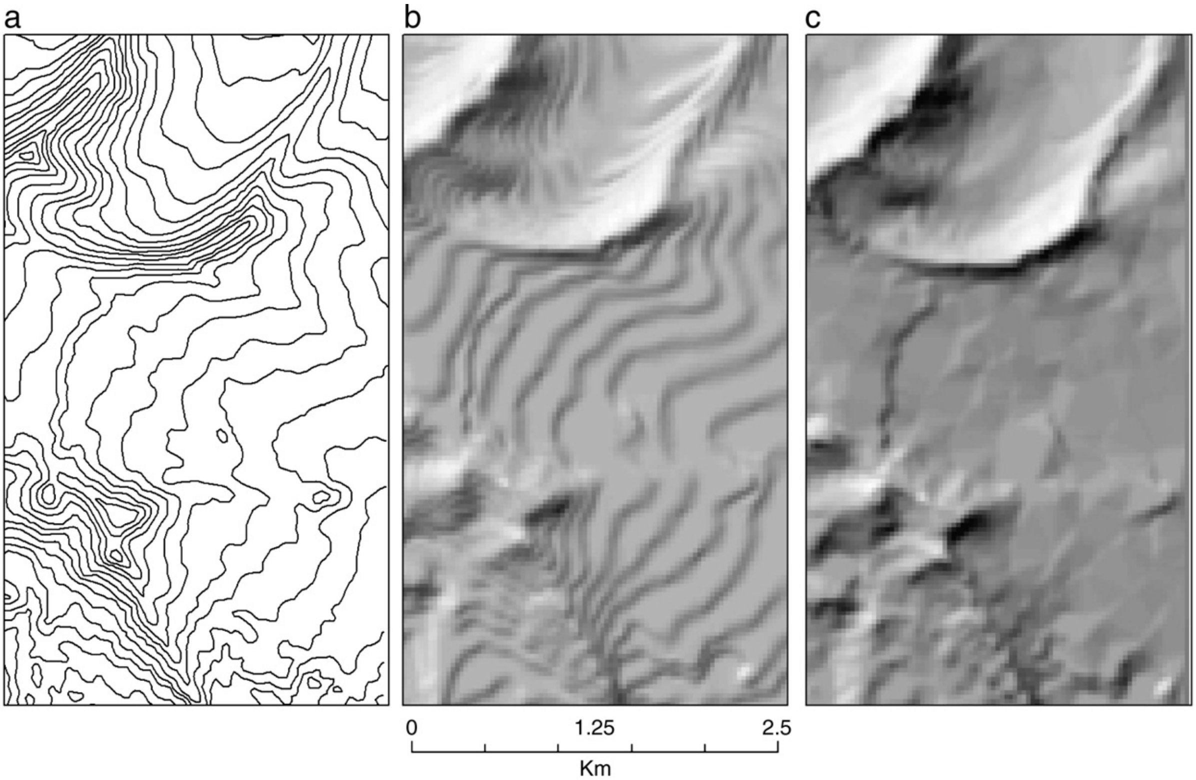

Fig. 3. The effect of interpolation methods on representation of terrain topography at a subsection of the study area. a) original contour lines, with 25 m interval; b) shaded relief map of the DEM created with the IDW method; c) shaded relief map of the TIN data structure.

methods such as IDW (Fig. 3b). Etzelmüller and Björnsson (2000) used the IDW interpolation method to create a continuous surface of glacier thickness. This systematic 'terracing' artifact was also reported in other glacier studies that used tension splines for surface representation (e.g. Mennis and Fountain, 2001). Terracing is known to affect subsequent calculations of topographic characteristics (slope, aspect and profile curvature) (Wilson and Gallant, 2000) which are of interest glaciological applications. For our study area, with gentle sloping terrain, the DEM created with the TOPOGRID algorithm yielded the smoothest surface. Minimal terracing is detected in this DEM, and appears as spikes on the histogram of elevation values (Fig. 4a).

Other glaciological studies (e.g. Gratton et al., 1990) preferred TIN's because of their advantage of capturing complex terrain variations, accurately representing ridges and streams, and reducing data redundancy on flat terrain (Burrough and McDonnell, 1998). For Coropuna, the TIN structure introduced noticeable triangular discretization on the gentle sloping lava flows and smooth glacier surface (Fig. 3c), which we considered unacceptable. Our results show that there are large differences in glacier surface representation by DEM's as a function of interpolation algorithm used. Based on minimizing both RMSEz and artifacts (terracing and triangulation), we chose the DEM created with the TOPOGRID algorithm (denoted as 'TOPO DEM') as the 1955 reference elevation dataset.

4.2. Accuracy assessment for the SRTM and ASTER — derived DEM's

SRTM elevations and ASTER elevations were checked against 64 GPS points from non-glaciated terrain. We focused on non-glaciated terrain to validate the DEM's because elevation changes might have occurred on the glacier between 1955 and 2000/2001. We present the elevation differences of the DEM's as RMSEz relative to the GPS points, and not the absolute vertical accuracy. The RMSEz of the SRTM DEM relative to the GPS points was 23.4 m. Since the vertical accuracy of GPS points is ~10 m (cf. Section 3.1), this gives an absolute vertical accuracy of 23.4 m±10 m. The specified SRTM accuracy standard is ±16 m for global coverage (Rabus et al., 2003). The frequency

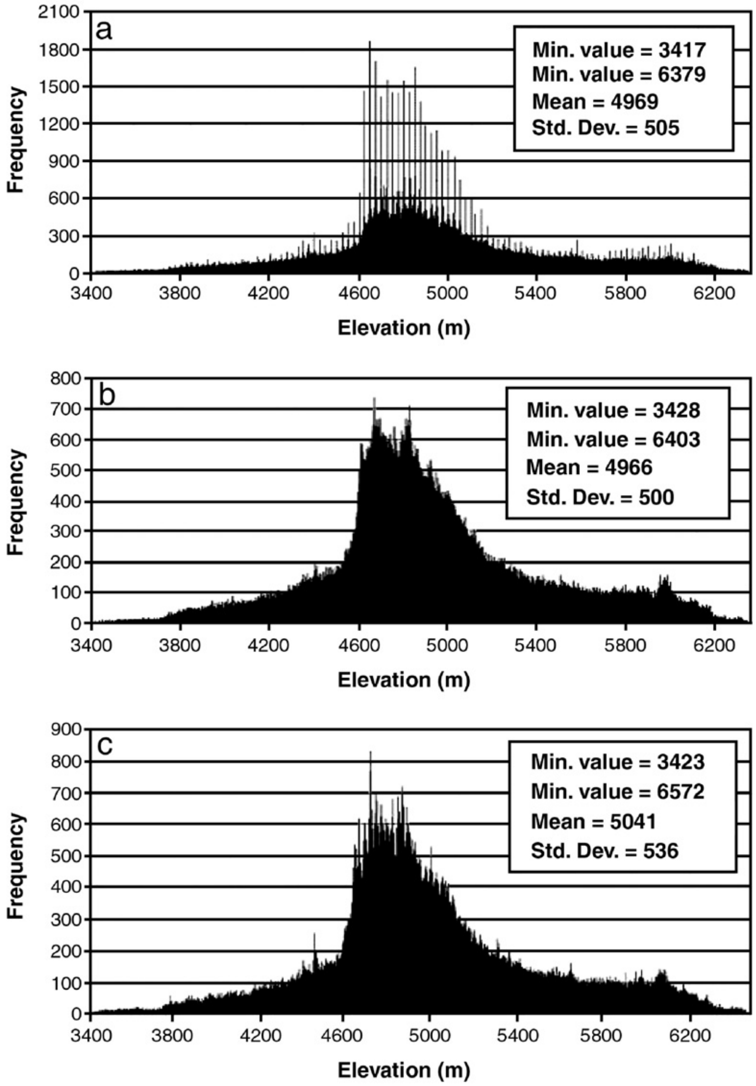

Fig. 4. Histograms of elevation values for the three DEM's analyzed. a) DEM created with TOPOGRID algorithm (TOPO DEM), b) SRTM DEM and c) ASTER DEM. Spikes on the elevation histograms represent elevation values along the contour lines used in the interpolation and point to the 'terracing' effect.

histogram of SRTM-derived elevations (Fig. 4b) indicates a normal distribution, with a few anomalously high values (spikes). Water bodies are not well defined and appear "noisy" or rough due to low radar backscatter (USGS, 2003). Height differences between SRTM elevations and GPS elevations tend to be randomly distributed (Fig. 5a), with SRTM elevations being both lower and higher than the GPS elevations.

The comparison of elevations from the ASTER DEM with GPS points shows both a large RMSEz and a vertical bias. The RMSEz of the ASTER DEM relative to the GPS points is 61.2 m. This corresponds to an absolute vertical accuracy of 61.2 m±10 m, which is bigger than the specified accuracy of 7–50 m for absolute ASTER DEM's (Lang and Welch, 1999). ASTER-derived elevations are consistently higher than the GPS points, and the magnitude of the vertical differences between ASTER and GPS increases with elevation along the GPS transects (Fig. 5b). Such vertical errors were reported in other studies. Kääb (2002) found an overall accuracy of ±60 m RMSEz when an absolute ASTER DEM was compared to a reference DEM on complex mountain terrain. However, better accuracy (±18 m RMSEz) was found at a section of moderate

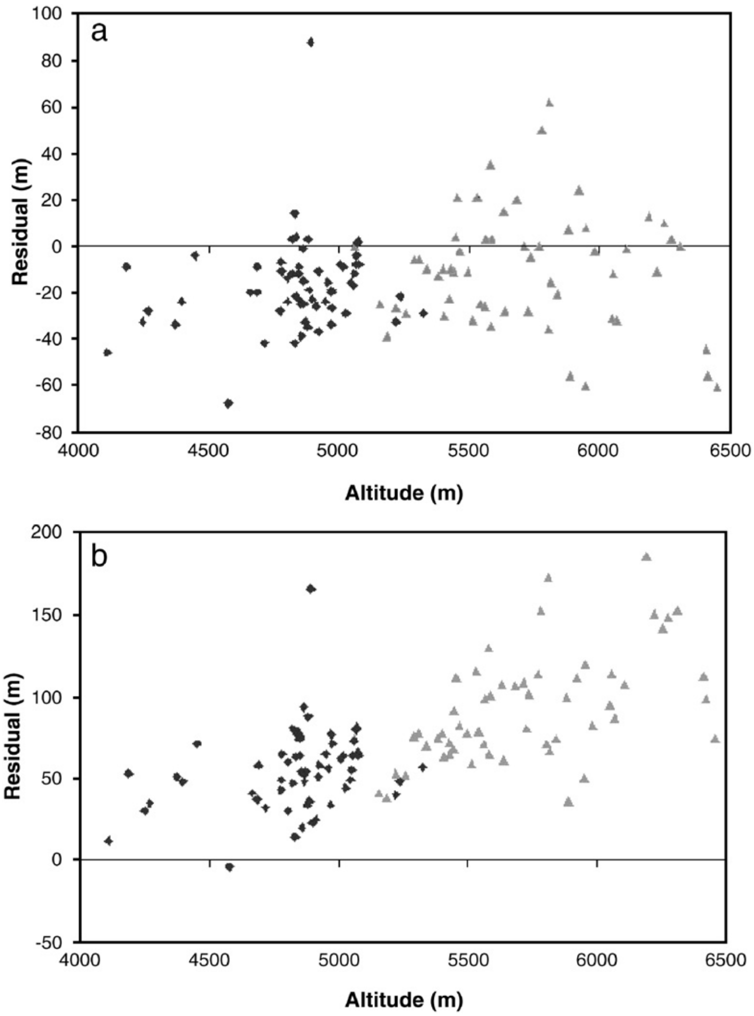

Fig. 5. Plots of height differences between the DEM's from satellite data and GPS elevation along GPS transects on non-glaciated (black diamonds) and glaciated areas (grey triangles). a) SRTM elevations minus GPS elevations; b) ASTER elevations minus GPS elevations.

topography in the same study (Kääb, 2002), suggesting that errors in the ASTER DEM's tend to increase in rugged mountain terrain.

Some errors come from some noise due to 'banding' in the ASTER L1A scene, visible in the DEM as spikes on the elevation histogram (Fig. 4c). Comparison of contours derived from the ASTER DEM with contours from topographic data revealed positional offsets as much as 300 m in *X* and 200 m in *Y*. These offsets were not consistent throughout the study area, pointing towards a distortion in the ASTER DEM in the *X* and *Y* coordinates. Such horizontal offsets have been observed at other study areas with high relief (Dwyer, LP DAAC Project Scientist, USGS EROS Data Center, personal communication). To correct the offsets, the ASTER DEM was fitted to the georeferenced ASTER L1A scene using a second order polynomial transformation based on 15 control points identified at lakes, stream crossings, and noticeable terrain features such as ridges.

Additional validations of the SRTM and ASTER-derived DEM's were performed by comparing their elevations with the reference 1955 DEM from topographic data on a cell-by-cell basis. Subtracting the reference DEM from the SRTM DEM yielded a mean difference of −1.8 m and a standard deviation of 15.7 m. The range of vertical differences was −113 m/+121 m, with the largest differences occurring on non-glaciates areas, at valley bottoms and sharp moraine ridges, as well as on a few flat areas where interpolation from contour lines produced erroneous values (either spikes or sinks).

Subtracting the reference DEM from the ASTER DEM yielded a mean difference of 80.5 m and standard deviation of 28.1 m. The range of differences was −86 m/ +500 m. The large positive differences

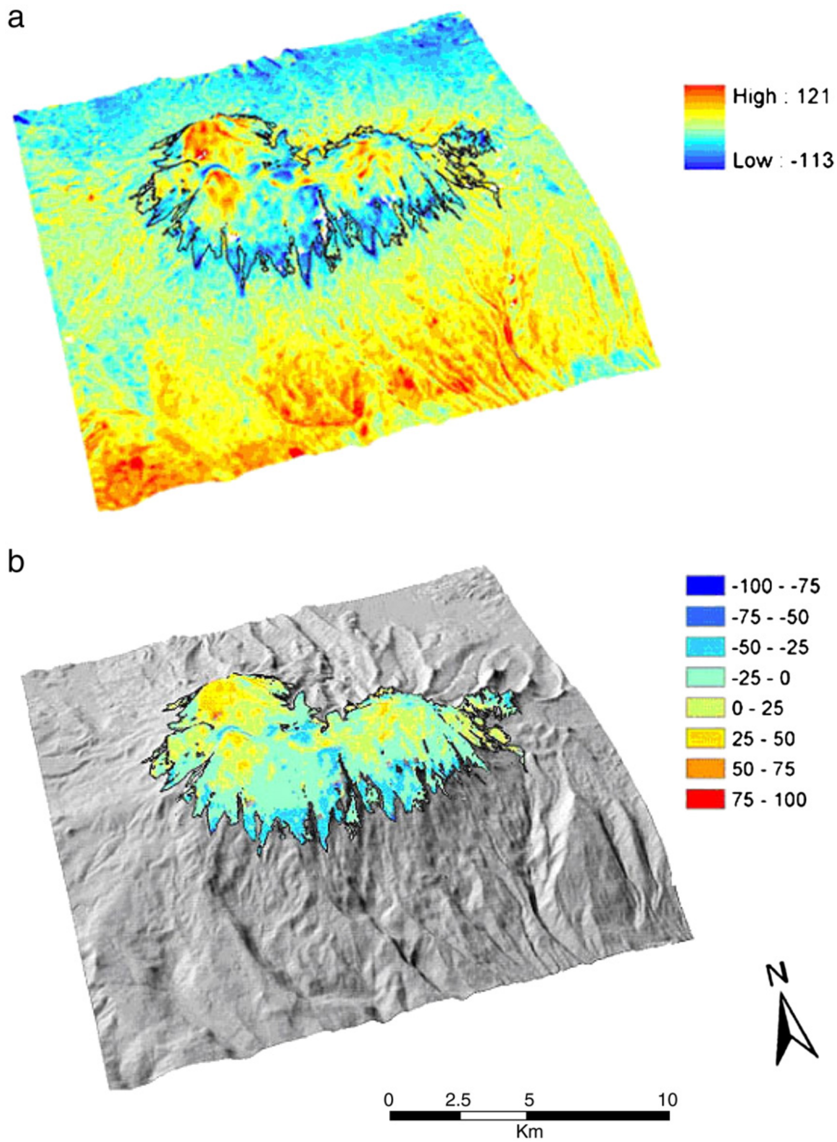

Fig. 6. Color maps of height differences (in meters) between the SRTM elevations and topographic elevations shown as 3D perspectives. a) 2000 SRTM DEM (before trend removal) minus 1955 TOPO DEM. The NE-SW spatial trend in elevation differences is visible. b) 2000 SRTM DEM (after trend removal) minus 1955 TOPO DEM. Areas depicted in white represent NODATA in the SRTM DEM. Also shown is the glacier extent obtained by classification of the October 2000 L1B ASTER scene (black line).

of +500 m come from 'spikes' of erroneous elevation values that occur on glaciated summits and sharp ridges. Such spikes of up to 500 m in ASTER DEM's were noted at other areas on sharp peaks (Kääb et al., 2002b). Elevation "waves" with about 200–300 m amplitude on low contrast glacier areas were also reported by the USGS EROS Data Center (Wessels, U.S. Geological Survey, Alaska Science Center, personal communication). These elevation errors are due to either steep northern slopes which are missed by the back-looking band 3b (Kääb et al., 2002b) or low contrast in the ASTER scenes over snow and ice, causing failure in the image-matching process (Toutin, 2002). While distortions in the ASTER DEM may be due to lack of adequate ground control points, in other studies in mountainous terrain, introducing more GCP's did not significantly remove this effect (Kääb et al., 2002b).

Height differences between the SRTM/ASTER DEM's and the reference DEM shown on color maps in Figs. 6a and 7a, indicate a systematic bias in both

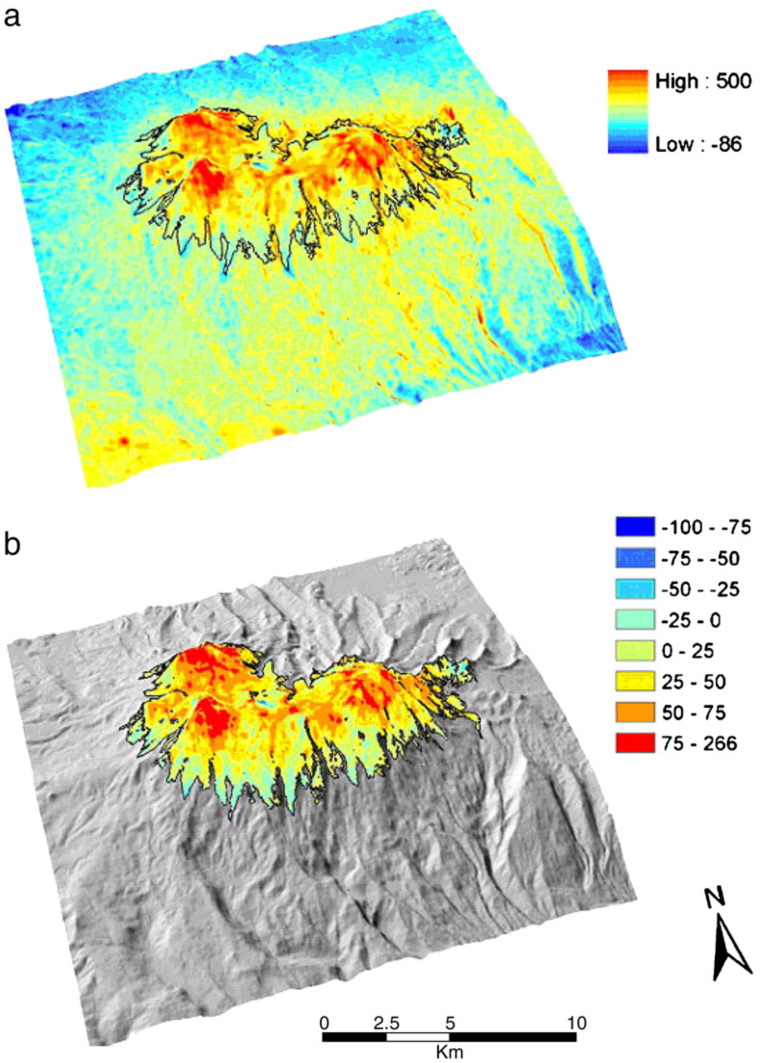

Fig. 7. Color maps of elevation differences (in meters) between ASTER DEM and the TOPO DEM's, in meters. a) 2001 ASTER DEM (before trend removal) minus 1955 TOPO DEM, with the NW-SE spatial trend visible; b) 2001 ASTER DEM (after trend removal) minus the 1955 TOPO DEM. Black lines represent the 2000 glacier extent derived from the ASTER scene.

difference maps, with positive residuals on non-glaciated areas in the north and negative residuals in lower valleys in the south. Similar biases in residuals were noted in other comparisons of ASTER DEM's with IGN topographic data (e.g. Vignon et al., 2003) as well as comparison of ASTER DEM's with photogrammetric-derived DEM's (Kääb et al., 2002b). We modeled the variation of residuals over the non-glaciated area for the two datasets by fitting various polynomial surfaces through the residuals. The best fit in terms of R-square was obtained by a first order polynomial, suggesting that the magnitude of the residuals increases linearly with location. The polynomial is derived by multiple regression on X and Y coordinates and is an inclined surface of the form:

$$f\{(x,y)\} = a_0 + a_1X + a_2Y,$$

where a_0 is the intercept and a_1 and a_2 are the slopes (Burrough and McDonnell, 1998).

The bias of elevation differences between the SRTM DEM and the reference DEM is a tilted surface, oriented towards the NNE (5.42°), which dips at a rate of 1.9 m vertical per 1 km northing, and has a range of −21 m to 20 m across the DEM. For the ASTER minus TOPO DEM, the bias is a tilted surface oriented towards the

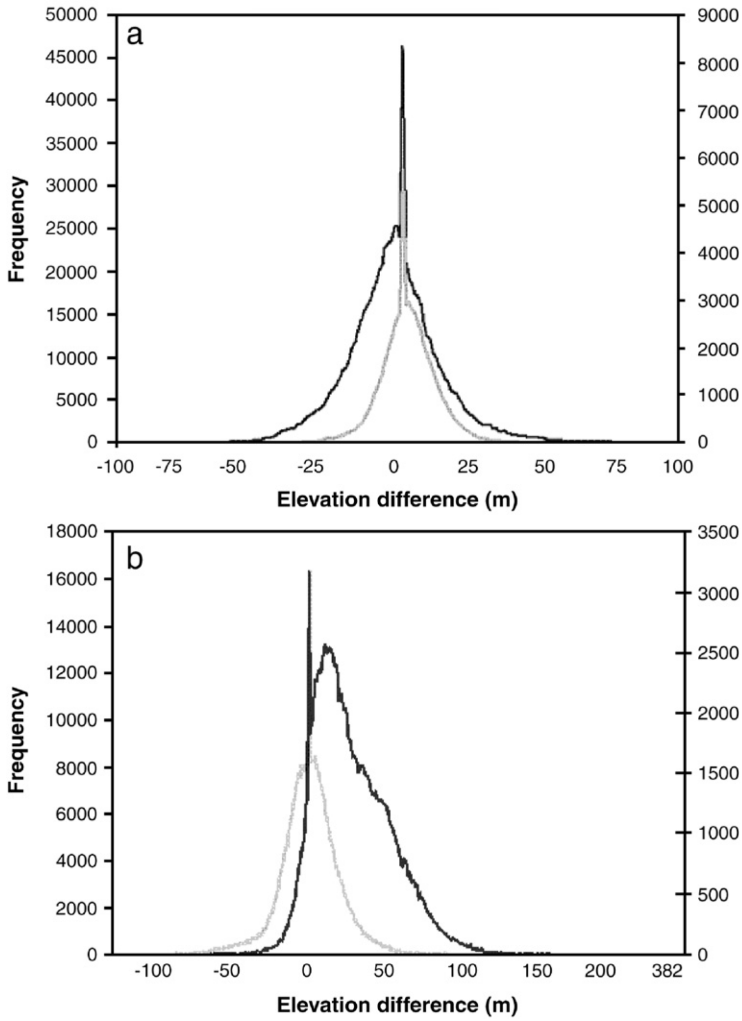

Fig. 8. Frequency histograms of elevation differences between the DEM's on non-glaciated (grey lines) vs. glaciated areas (black lines), after the trend removal. a) SRTM DEM minus TOPO DEM; b) ASTER DEM minus TOPO DEM.

NNW (349.30°), which dips at a rate of 2 m vertical per 1 km northing, and has a range of 47 m to 96 m across the DEM.

Once the trend was removed, the mean statistics for the elevation differences on non-glaciated areas yielded:

SRTM DEM minus TOPO DEM (Fig.8a): mean = 0, std. deviation = 9.5 m
ASTER DEM minus TOPO DEM's (Fig. 8b): mean = 0, std. deviation = 20.6 m.

The histograms of elevation differences on non-glaciated areas are close to normally distributed (Fig. 8 a–b). Large standard deviations on non-glaciated areas point to artifacts in the DEM's (high or low values) and they do not affect subsequent analysis of the glaciated areas.

After the trend removal, we examined the effect of slope and aspect on the vertical differences between the DEM's. Correlations with slope yielded a coefficient (Pearson's r) of 0.54 for SRTM minus reference DEM and 0.69 for ASTER minus the reference DEM. The plots of vertical differences with respect to slope (Fig.9) show that elevation errors in the SRTM and ASTER DEM's tend to increase with slope. On slopes less than 45°, there is almost no difference in SRTM-derived elevations and the topographic DEM, but corresponding ASTER elevations are consistently higher than the reference DEM. For the SRTM DEM, elevation errors of up to −25/+50 m occur on 60–65° slopes. For the

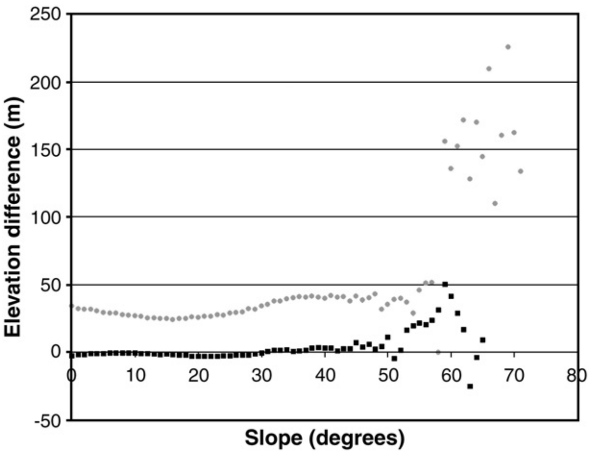

Fig. 9. Vertical differences between DEMs from satellite data and DEM from topographic data as a function of terrain slope: SRTM minus TOPO DEM (black squares) and ASTER minus TOPO DEM (grey dots). Largest vertical differences between SRTM/ASTER and the topographic DEM occur on steepest slopes.

ASTER DEM, elevation errors greater than 100 m occur on steep slopes (60–77°) and correspond to the 'spike' artifacts in the ASTER DEM. These results are consistent with trends noted in ASTER-derived DEM's. For instance, Kääb (2002) and Kääb et al. (2002b) found large vertical differences in the ASTER DEM's compared to reference DEM's from topographic data at steep slopes.

Vertical differences between the SRTM DEM and the reference DEM (Fig. 10a) do not depend on slope aspect. The mean elevation differences between SRTM and reference DEM range from −5 m on S-facing slopes to 1 m on NNE-facing slopes. The ASTER DEM displays bigger mean vertical differences ranging from −3 m on W-facing slopes to +19 m on E-facing aspects (Fig. 10b). We expected bigger elevation errors on N-facing slopes, which are normally missed by the back-looking band 3b (Kääb et al., 2002b). For instance, decreased vertical accuracy of ASTER DEM's on northern slopes was reported by Kääb (2002) and Kääb et al. (2002b). Our results show that mean errors tend to occur on aspects between 0 and 180°, not only on N-facing slopes. This suggests that the large vertical errors in the ASTER DEM cannot be entirely explained by the back-looking ASTER channel.

4.3. Glacier signal from the SRTM DEM

We checked elevations from the SRTM and ASTER DEM's against GPS points on glaciated areas. The difference between SRTM elevations and 56 GPS elevations acquired on the glaciated area yielded a RMSEz of 27 m, which is ~4 m bigger than on non-glaciated areas. SRTM elevations are both higher and lower than the GPS points on the glacier (Fig. 5a). The RMSEz of ASTER elevations with respect to GPS points on the glacier was 98 m, and residuals increase with altitude (Fig 5b). This large vertical bias

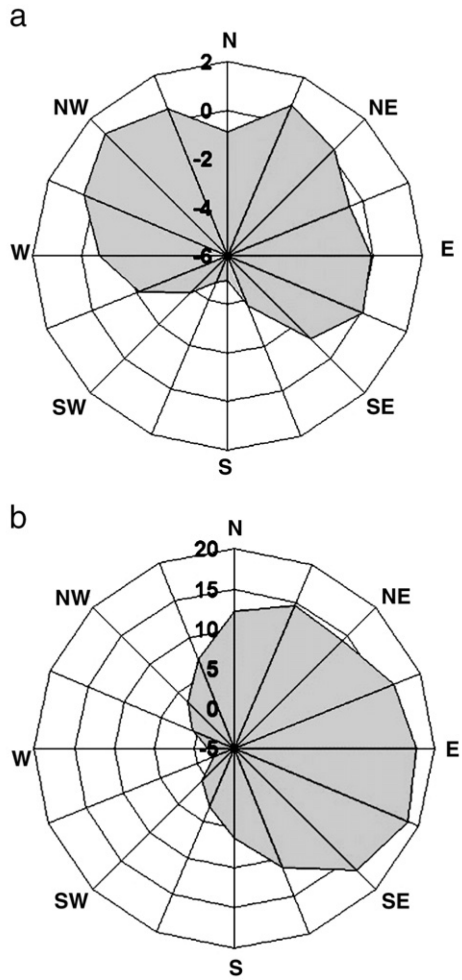

Fig. 10. Radar charts of vertical differences between the DEM's as a function of aspect. a) SRTM DEM minus TOPO DEM; b) ASTER DEM minus TOPO DEM.

Table 2
Statistics summary of map differences for the glaciated areas vs. non-glaciated areas after trend removal

Statistics	SRTM — TOPO DEM (m)		ASTER — TOPO DEM (m)	
	Glaciated	Non-glaciated	Glaciated	Non-glaciated
Mean	−5	0.0	28.5	0.0
Std. deviation	15.8	9.5	26	20.5

implies that the ASTER DEM, created with a limited number of GCP's, is not suitable for glaciological interpretation.

To quantify the glacier signal from the SRTM DEM, we examined the mean elevation differences (SRTM minus topographic DEM) on glaciated areas after removing the NNE-SSW spatial trend. Once the trend was removed, the elevation differences on the glaciated area were negatively skewed (Fig. 8a), with a mean of −5 m and a standard deviation of 15.8 m (Table 2). We consider the remaining mean difference of −5 m±15.8 m as a signal of glacier thinning (95% confidence interval). Average height differences between the SRTM and topographic DEM on the glaciated area increase with altitude, with a correlation coefficient (Pearson's *r*) of 0.62 (Fig. 11a). Cell-by-cell comparison of elevations from SRTM data with topographic DEM within the glaciated area (Fig. 6b) show ablation at the toes of the glaciers (−25 m to −75 m surface lowering) along with an apparent thickening at the summits (25–50 m). Similar comparisons of ASTER data to topographic data in Cordillera Blanca (Peru) revealed a loss of altitude of as much as −23 m at the glacier toes (Vignon et al., 2003). Ablation in the lower parts of the glaciers (via ice melting and sublimation) was also observed from field measurements in other tropical glaciers (Kaser et al., 1990; Kaser, 1999).

Thickening in the accumulation zone of the glaciers is a less common trend and was observed in some mountain glaciers around the world during the 1961–1997 time period (Dyurgerov and Meier, 2000). However, in the climatic context of Coropuna, an average thickening of 25–50 m firn in 50 yr, or 0.5 m/yr would represent a mean increase in precipitation of 250–

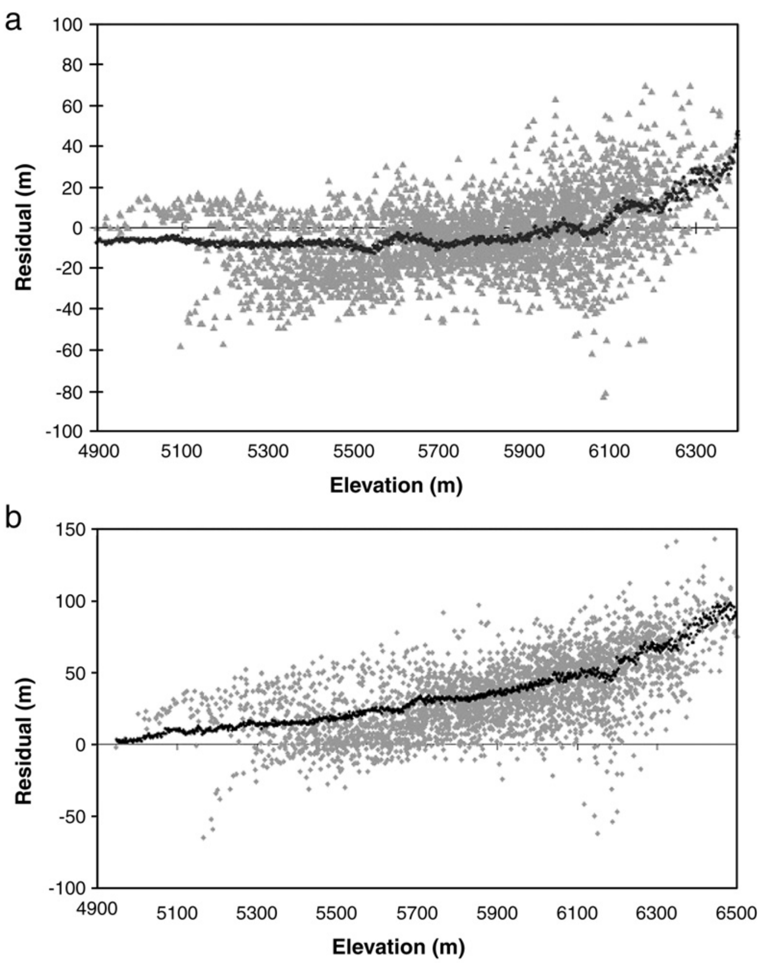

Fig. 11. Vertical differences between the DEM's as a function of altitude on the glaciated area averaged in a 150×150 m neighborhood (grey symbols). Also shown are mean trends calculated as average difference in 2 m elevation bands (black dots). a) SRTM DEM minus TOPO DEM; b) ASTER DEM minus TOPO DEM.

500 mm water equivalent. At the col, our results agree with field data from the ice core drilling of June 2003, which also point to an accumulation of 0.5–1 m firn / yr in the col (Ginot, Laboratoire de Glaciologie et Geophysique de l'Environnement, Grenoble, personal communication). However, at the summits, the increase of 0.5–1 m firn/yr from the DEM comparison is 2–4 times bigger than ice core results (.26 m firn/yr) (Ginot, Laboratoire de Glaciologie et Geophysique de l'Environnement, personal communication). In the upper part of the glaciated area the noise may be too high to be able to infer a positive change of 25–50 m in altitude.

The elevation differences between ASTER elevations and reference DEM on glaciated area are positively skewed (Fig. 8b), with a mean of 28.5 m and a standard deviation of 26 m. Comparison of GPS points with corresponding ASTER elevations on glaciated areas (Fig. 5b) shows that the ASTER DEM is too high on glaciated terrain, with a RMSEz error of 98.3 m with respect to GPS points. The ASTER DEM is also systematically higher than the topographic DEM (Fig. 11b). However, an examination of cell-by-cell differences between the ASTER DEM and the reference DEM (Fig. 7b) shows negative residuals (−50 to −25 m) in the ablation areas of the southern glaciers. While surface lowering at the glacier toes is consistent with results from the SRTM DEM, we could not quantify the glacier signal from the ASTER DEM due to the altitudinal bias and the large elevation 'spikes' on the glacier surface, which are affecting the mean statistics. We suspect that the large elevation spikes were due to lack of contrast over the glacier in the ASTER image. The VNIR and SWIR gain level settings, which are based on sun angle, can be optimized for snow targets to provide maximum contrast over ice and snow (Raup et al., 2000). However, the ASTER images currently available for Coropuna were not acquired with these settings and therefore provided little contrasts over the glacierized surface.

4.4. Changes in glacier extent and volume

For 1962, Ames et al. (1989) reported a glaciated area of 82.6 km^2 on Nevado Coropuna based on planimetric analysis of 1962 aerial photography. Based on the ASTER L1B scene from October 2000, we obtained a glacier area of 60.8 km^2, which represents a loss of 26% in glacier area from 1962 to 2000. Our results are consistent with glacier retreat observed in Cordillera Ampato during the last few decades. Ames et al. (1989) reported a total glaciated area of 146.7 km^2 based on 1962 aerial photography. The total glaciated area in the Ampato range was estimated to be 105 km^2 based on Landsat TM imagery (Morales-Arnao, 1999). This corresponds to a retreat of 27% in Cordillera Ampato from 1962 to the end of the 20th century. Glacial retreat in Peru has also been observed in other areas, especially in Cordillera Blanca (Kaser et al., 1990; Hasternath and Ames, 1995; Georges, 2004).

5. Conclusions and further applications

Using DEM's derived from topographic and satellite data at different steps in time holds potential for glacier analysis. DEM's constructed from old topographic data still constitute a valid elevation dataset for comparison with more recent DEM's for glaciology purposes. Here we created a DEM from 1:50,000 topographic data for Nevado Coropuna and tested different interpolation techniques. Based on RMSEz and visual analysis, the TOPOGRID algorithm was found to be superior to the other techniques examined, with the smallest RMSEz error and least interpolation artifacts.

Error analyses were performed on all DEM's to characterize the bias present in the various DEM's. We removed the spatial bias to distinguish a glacier signal. We found that the SRTM dataset with a RMSEz of 23.4 m ± 10 m was suitable for glaciological applications after some calibration. However, in areas of rugged terrain, the SRTM resolution (90 m) was not sufficient to accurately represent the topography. Comparison of the 2000 SRTM DEM with the DEM from 1955 topographic data points to an average thinning of ~5 m on the glacier surface, with a significant lowering of the glacier surface at the glacier toes and an apparent accumulation on the summits. We attribute the vertical differences of more than 25 m at the summits to possible errors in either the SRTM data or the topographic data at higher elevations and steeper slopes. While lowering of glacier surface at the toes was visible in the ASTER DEM, large elevation errors and altitudinal bias did not allow quantifying a glacier signal from the ASTER data.

In conclusion, the analysis of multi-temporal DEM's to quantify glacier changes is extremely sensitive to the quality and spatial resolution of the DEM's. For our study of glacier change using DEM's on Nevado Coropuna, we found that several steps were necessary: referencing all elevation data to the same vertical datum; evaluation of DEM differences in non-glaciated areas; testing the DEM's against field GPS survey points;

visualization techniques such as shaded relief, slope angle and comparison of contours; removing the biases in the elevation datasets.

Future steps to minimize large error differences occurring in DEM's derived from satellite data include filtering and smoothing of the DEM's (Toutin, 2001, 2002; Hirano et al., 2003). These techniques may help to better distinguish and quantify glacier surface changes.

Acknowledgments

The research was supported by the NSF/IGERT — sponsored graduate training program entitled Carbon, Climate and Society Initiative (CCSI) at University of Colorado. The French program ACI "Observation de la Terre" supported the use of remote sensing for glaciological studies. The Niwot Ridge LTER project provided logistical support (NSF DEB 9810218). We thank the GLIMS team for facilitating free access to the ASTER data through the NASA ESE Pathfinder project; USGS EROS data center for provinding the ASTER and SRTM data; Bernard Pouyaud and Bernard Francou (UR GREAT ICE, IRD France) for supporting the participation of the main author in the ice core drilling expedition on Coropuna; the Glaciology Unit at INRENA, Huaraz, for providing helpful assistance; the UNAVCO facility in Boulder for assisting with GPS corrections.

References

Ackerman, T., Erickson, T., Williams, M.W., 2001. Combining GIS and GPS to improve our understanding of the spatial distribution of snow water equivalence (SWE). Proceedings of ESRI USERS Conference, San Diego, CA.

Ames, A., Muñoz, G., Verástegui, J., Zamora, M., Zapata, M., 1989. Glacier Inventory of Peru. Part I. Hidrandina S.A. Unit of Glaciology and Hydrology. Huaraz-Perú.

Aniya, M., Sato, H., Naruse, R., Skvarca, P.C.G., 1996. The use of satellite and airborne imagery to inventory outlet glaciers of the Southern Patagonia Icefield, South America. Photogrammetric Engineering and Remote Sensing 62, 1361–1369.

Berthier, E., Arnaud, Y., Baratoux, D., Vincent, C., Rémy, F., 2004. Recent rapid thinning of the "Mer de Glace" glacier derived from satellite optical images. Geophysical Research Letters 31, L17401. doi:10.1029/2004GL020706.

Burrough, P.A., McDonnell, R.A., 1998. Principles of Geographic Information Systems. Oxford University Press, Oxford.

Cogley, J.G., Jung-Rothenhausler, F., 2004. Uncertainty in digital elevation models of Axel Heiber Island, Arctic Canada. Arctic, Antarctic and Alpine Research 36 (2), 249–260.

Duncan, C.C., Klein, A.J., Masek, J.G., Isacks, B.L., 1998. Comparison of late Pleistocene and modern glacier extents in central Nepal based on digital elevation data and satellite imagery. Quaternary Research 49, 241–254.

Dyurgerov, M.B., Meier, M.F., 2000. Twentieth century climate change: evidence from small glaciers. PNAS 97 (4), 1406–1411.

Etzelmüller, B., 2000. On the quantification of surface changes using grid-based digital elevation models (DEMs). Transactions in GIS 4 (2), 129–143.

Etzelmüller, B., Björnsson, H., 2000. Map analysis techniques for glaciological applications. International Journal of Geographical Information Science 14 (6), 567–581.

Etzelmüller, B., Vatne, G., Odegard, R.S., Sollid, J.L., 1993. Mass-balance and changes of surface slope, crevasse and flow pattern of Erikbreen, Northern Spitsbergen – an application of a geographical information-system (GIS). Polar Research 12 (2), 131–146.

Falorni, G., Istanbulluoglu, E., Bras, R.L., 2003. A method for improving SRTM DEMs in high-relief terrain. EOS Transactions AGU 84 (46).

Georges, C., 2004. 20th century glacier fluctuations in the Cordillera Blanca (Perú). Arctic, Antarctic, and Alpine Research 36 (1), 100–107.

Gratton, D.J., Howarth, P.J., Marceau, D.J., 1990. Combining DEM parameters with Landsat MSS and TM imagery in a GIS for mountain glacier characterization. IEEE Transactions on Geoscience and Remote Sensing 28 (4), 766–769.

Hasternath, S., Ames, A., 1995. Recession of Yanamaery glacier in Cordillera Blanca, Perú during the 20th century. Journal of Glaciology 41 (137), 191–196.

Hirano, A., Welch, R., Lang, H., 2003. Mapping from ASTER stereo image data: DEM validation and accuracy assessment. ISPRS Journal of Photogrammetry and Remote Sensing 57 (5–6), 356–370.

Hutchinson, M.F., 1988. Calculation of hydrologically sound digital elevation models. Proceedings of Third International Symposium on Spatial Data Handling, Sydney.

Kääb, A., 2002. Monitoring high-mountain terrain deformation from repeated air- and spaceborne optical data: examples using digital aerial imagery and ASTER data. ISPRS Journal of Photogrammetry and Remote Sensing 57 (1–2), 39–52.

Kääb, A., Paul, F., Maisch, M., Hoelzle, M., Haeberli, W., 2002a. The new remote sensing-derived Swiss glacier inventory: II. First results. Annals of Glaciology 34, 362–366.

Kääb, A., Huggel, C., Paul, F., Wessels, R., Raup, B., Kieffer, H., Kargel, J., 2002b. Glacier monitoring from ASTER imagery: accuracy and applications. Proceedings of EARSeL LIS-SIG Workshop, Berne, March 11–13, 2002.

Kaser, G., 1999. A review of modern fluctuations of tropical glaciers. Global and Planetary Change 22, 93–103.

Kaser, G., Ames, A., Zapata, M., 1990. Glacier fluctuations and climate in the Cordillera Blanca, Perú. Annals of Glaciology 14, 136–140.

Khalsa, S.J.S., Dyurgerov, M., Khomova, T.B.R., Barry, R.G., 2004. Space-based mapping of glacier changes using ASTER and GIS tools. IEEE Transactions on Geoscience and Remote Sensing, 42 (190), 2177–2183.

Klein, A.G., Isacks, B.L., 1996. Glaciers: tracking change in the central Andes Mountains. GIS World 9, 48–52.

Lang, H.R., Welch, R., 1999. Algorithm Theoretical Basis Document for ASTER Digital Elevation Models, Version 3.0. Jet Propulsion Laboratory, Pasadena, CA. 69 pp.

Mennis, J.L., Fountain, A.G., 2001. A spatio-temporal GIS database for monitoring alpine glacier change. Photogrammetric Engineering and Remote Sensing 67 (8), 967–975.

Morales-Arnao, B., 1999. Glaciers of Peru. In: Williams Jr., R.S., Ferrigno, J.G. (Eds.), Satellite image atlas of glaciers of the world:

South America. United States Geological Survey Professional Paper 1386-I. United States Government Printing Office, Washington.

Paul, F., 2001. Evaluation of different methods for glacier mapping using Landsat TM. Proceedings of EARSeL Workshop on Remote Sensing of Land Ice and Snow, Dresden, June 16 -17, 2000, vol. 1, pp. 239–245.

Paul, F., Kääb, A., Maisch, M., Kellenberger, T., Haeberli, W., 2002. The new remote- sensing-derived Swiss glacier inventory: I. methods. Annals of Glaciology 34, 355–361.

Rabus, B., Eineder, M., Roth, A., Bamler, R., 2003. The shuttle radar topography mission—a new class of digital elevation models acquired by spaceborne radar. ISPRS Journal of Photogrammetry and Remote Sensing 57 (4), 241–262.

Rapp, R.H., 1996. Use of potential coefficient models for geoid undulation determination using a spherical harmonic representation of the height anomaly/geoid undulation difference. Journal of Geodesy 71 (5), 282–289.

Raup, B.H., Kieffer, H.H., Hare, T.M., Kargel, J.S., 2000. Generation of data acquisition requests for the ASTER satellite instrument for monitoring a globally distributed target: glaciers. IEEE Transactions on Geoscience and Remote Sensing 38, 1105–1112.

Rentsch, H., Welsch, W., Heipke, C., Miller, M., 1990. Digital terrain models as a tool for glacier studies. Journal of Glaciology 36 (124), 273–278.

Rivera, A., Casassa, G., 1999. Volume changes on Pio XI glacier, Patagonia: 1975–1995. Global and Planetary Change 22 (1–4), 233–244.

Sidjak, R., 1999. Glacier mapping of the Illecillewaet icefield, British Columbia, Canada, using Landsat TM and digital elevation data. International Journal of Remote Sensing 20 (2), 273–284.

Toutin, T., 2001. Elevation modeling from satellite visible and infrared (VIR) data. International Journal of Remote Sensing 22 (6), 1097–1125.

Toutin, T., 2002. Three-dimensional mapping with ASTER stereo data in rugged topography. IEEE Transactions on Geoscience and Remote Sensing 40 (10), 2241–2247.

USGS, 2003. SRTM documentation. Available at: ftp://edcsgs9.cr.usgs.gov/pub/data/srtm/Documentation/ (accessed May 16, 2003).

Vignon, F., Arnaud, Y., Kaser, G., 2003. Quantification of glacier volume change using topographic and ASTER DEMs: a case study in the Cordillera Blanca. Proceedings of Geoscience and Remote Sensing Symposium, IEEE International 4, 2605–2607.

Welch, R., Jordan, T., Lang, H., Murakami, H., 1998. ASTER as a source for topographic data in the late 1990's. IEEE Transactions on Geoscience and Remote Sensing 36 (4), 1282–1289.

Wilson, J.P., Gallant, J.C., 2000. Digital terrain analysis. In: Wilson, J.P., Gallant, J.C. (Eds.), Terrain analysis - principles and applications. Wiley, New York.

Wood, J.D., Fisher, P.F., 1993. Assessing interpolation accuracy in elevation models. IEEE Computer Graphics and Applications 13 (2), 48–56.